International Journal of Microwave and Wireless Technologies

cambridge.org/mrf

A robust and efficient wall parameter estimation approach for through wall radar

Akhilendra Pratap Singh[1,2]

[1]Department of Electronics Engineering, Indian Institute of Technology (Banaras Hindu University), Varanasi, U.P., India and [2]School of Engineering and Technology, Maharishi University of Information Technology, Lucknow, U.P., India

Research Paper

Cite this article: Singh AP (2023). A robust and efficient wall parameter estimation approach for through wall radar. *International Journal of Microwave and Wireless Technologies* **15**, 1147–1153. https://doi.org/10.1017/S1759078722001131

Received: 20 June 2022
Revised: 21 September 2022
Accepted: 22 September 2022

Key words:
Artificial neural network; transmission line method; wall parameter estimation

Author for correspondence:
Akhilendra Pratap Singh,
E-mail: apsingh.rs.ece14@itbhu.ac.in

Abstract

In through-wall radar system, the wall parameters, including permittivity, and wall thickness are of crucial importance for locating targets precisely. Recently, to obtain a quick and accurate estimation of wall parameters, an approach based on machine learning was introduced. However, these approaches are less reliable as only simulations results are presented. One of the major concerns with machine learning-based approaches is the generation of training and testing data which require fabrication of wall with different permittivity, thickness, and conductivity. Creating walls with different permittivity, thickness, and conductivity can really be challenging and expensive. Therefore, an effort has been made in this paper to establish a cost-effective and robust machine learning-based wall parameter estimation process with the usage of transmission line method and artificial neural network. The implementation and efficacy of proposed approach have been demonstrated through simulation and experimental results. The proposed approach quickly and accurately predicted the wall relative permittivity and thickness of real building wall. The merit of proposed approach is that it is less complex and computational efficient as it can extract wall parameters from only one measurement and therefore can be used in conjunction with any commercial through-wall radar systems.

Introduction

Through-wall radar systems (TWRS) are a new non-destructive technology that can detect and locate targets hidden behind a wall. TWRS can only locate the target if the exact wall parameters are known in advance. Ambiguities in wall parameters can cause the target image to defocus and shift away from its true location [1]. Therefore, estimating exact wall parameters is critical in real environment when there is access from the side of the wall.

In this regard, a number of researchers have presented their works. In general, there are four different types of wall parameter estimate methods. The first is the trajectory intersection method, which requires multiple measurements to be taken at varying standoff distances with an array structure [2]. This method appears sophisticated and difficult to perform in a real-world scenario because of the various measurements. The time-delay estimation approach likewise needs at least two experiments to be run. The method calculates the parameters by measuring the time delay caused by various antenna spacings [1, 3]. The second method is autofocussing, in which behind-the-wall images are created using various wall characteristics and an image focusing metric is derived [4–6]. The wall parameter is calculated by looking for a better-quality focusing metric. It is computationally expensive and time demanding because it employs an iterative optimization strategy. The third is a pole extraction approach based in which the wall parameter can be estimated from frequency domain signal [7]. This method provides quick and precise estimates, but it requires the need for measurement to be performed by removing the wall to eliminate unwanted received signal other than the wall so that received signal contains information about walls only, which limits its usefulness in practice. The fourth is a machine learning-based method in which an SVM-based regression model is created to build a relationship between scattered field and wall parameters [8–10]. Deep learning models have also been introduced for simultaneous estimation of wall parameters and target location [11–13]. These models have shown to yield quick and highly accurate results, but are less reliable as only simulation results are shown. In addition, these models have shown to be effective for the case of a single and double target, but this approach is not suitable for the case of multiple targets. A comparison between different machine learning methods is described in Table 1.

Differing to the method above, this paper introduces a cost-effective machine leaning-based wall parameter estimation approach. The permittivity of the wall is influenced by the moisture content and humidity, both of which are unknown and unexpected. One of the major concerns with machine learning-based approaches is the generation of training and testing data which require fabrication of wall with different permittivity, thickness, and conductivity.

Table 1. Comparison of machine learning-based wall parameter estimation methods

Reference	Machine learning methods	Main contribution	Accuracy	Computational complexity [14]
[8]	Support vector machine	Wall parameters estimation	High	Medium $O(DN_{tr}^2 + N_{tr}^3 I)$
[9]	Support vector machine	Wall parameters estimation	High	Medium $O(DN_{tr}^2 + N_{tr}^3 I)$
[10]	Least square support vector machine	Wall parameters estimation	High	Medium $O(DN_{tr} + N_{tr}^2)$
[11, 12]	Deep neural network	Simultaneous wall parameters estimation and target localization	High	High $O(DN_{tr}IL)$
[13]	Convolution neural network	Simultaneous wall parameters estimation and target localization	High	High $O(DN_{tr}IL)$
Proposed	Single hidden layer dense neural network	Wall parameter estimation	High	Low $O(DN_{tr}I)$

Note: N_{tr} is the number of training instances, D is the dimensionality of data, I is the number of iterations and L is the number of layers for neural networks.

Creating walls with different permittivity, thickness, and conductivity can really be challenging and expensive. Therefore, an effort has been made in this paper to establish a cost-effective (i.e. fabrication complexity, time complexity, and cost) and robust wall parameter estimation process with the usage of transmission line method and artificial neural network (ANN). ANNs were initially introduced to classify and recognize targets from radar images [15, 16]. Recently, ANN has also been used in radar applications to resolve regression problems, such as soil moisture prediction [17]. This research incorporates ANN into TWRS to estimate the wall characteristics, drawing inspiration from these effective implementations. In general, a larger neural network with more weights and hidden nodes may be more effective at problem-solving but require much greater computational resources and longer training times. Therefore, in this paper, we have considered smaller neural network architecture that needs shorter training time and have less network complexity thereby can be useful in real-time environment where speed is essential. The performance of artificial neural network trained with dataset of synthetic through-wall imaging (TWI) signal generated from an equivalent transmission-line circuit model has been demonstrated. Instead of creating separate regression functions for each parameter and estimating each parameter by its own function, a two-stage ANN model is used to leverage the estimated results of one parameter for the estimation of the other parameter. The implementation and efficacy of proposed method have been demonstrated through simulation and experimental results. The proposed method is computationally efficient and provides accurate results. The result of the paper is organized as follows. Section "Analytical transmission line modeling of wall radar return" describes analytical transmission line modeling of wall radar return. Section "Proposed method for wall parameter estimation" presents the proposed method for wall parameter retrieval. Section "Implementation of ANN with simulation and experimental validation" reports and discusses the experimental results. Section "Conclusion" presents the conclusions.

Analytical transmission line modeling of wall radar return

As shown in Fig. 1, consider a homogeneous smooth wall made of N layers sandwiched between two semi-infinite media, A and B. Each layer of the wall has a thickness *di* and is infinitely long in x and y directions but finite in z. Allow an electromagnetic wave transmitted from an antenna placed at a certain standoff

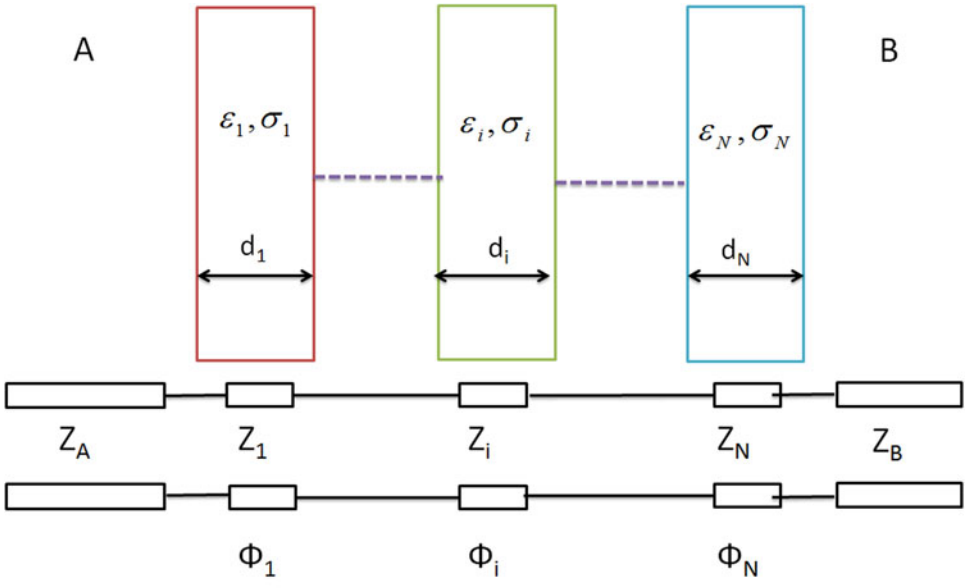

Fig. 1. Section view of a multilayer media consisting of N layers between two semi-infinite mediums and its equivalent transmission line model.

https://doi.org/10.1017/S1759078722001131 Published online by Cambridge University Press

distance to illuminate the wall. The electromagnetic wave in a uniform plane is normally incident on the wall from medium A. The electric and magnetic field components of the wave are orthogonal to the propagation direction z, and thus the incident plane wave is a TEM one.

The incident wave travels through the layers of the wall at varying phase velocities, and some of the energy is reflected and some is transmitted at each interface. The propagation of a wave along layers of wall can be described by electromagnetic field theory as the propagation of a TEM wave along cascaded transmission line sections, the crucial parameters being the characteristic impedances Z and the propagation constants [18]. These parameters change as the layer's permittivity changes.

The frequency response of the N layers of wall can be evaluated using the analogy shown in Fig. 1 by solving the corresponding circuit equations.

In Fig. 1, the i^{th} transmission line segment characteristic impedance and electrical length can be written as [18]:

$$Z_i = \frac{Z_0}{\sqrt{\varepsilon_r}} \tag{1}$$

$$\phi_i = \beta_i d_i \tag{2}$$

where,

Z_0 is the vacuum's characteristic impedance, ε_r is the layer's relative electric permittivity, and β_i is the propagation constant in the layer.

The propagation constant is proportional to the incident field's angular frequency as follows [18]:

$$\beta_i = \frac{\omega}{c}\sqrt{\varepsilon_r} \tag{3}$$

where c is the speed of light in vacuum, and ω is the angular frequency of monochromatic incident field.

Let E_i represent the electromagnetic (EM) field that illuminates the wall. The reflected and transmitted signals from the N transmission line sections can be related to the incident signal using the reflection and transmission coefficients, which are based on well-established microwave circuit theory. The 2×2 matching matrix [MM] and propagation matrix [PM] of any layer must be evaluated in order to relate the reflected and transmitted signals to the incident signal [18]:

$$[PM]_i = \begin{bmatrix} e^{-j\phi_i} & 0 \\ 0 & e^{-j\phi_i} \end{bmatrix} \tag{4}$$

$$[MM]_{i,i+1} = \frac{1}{\tau_{i,i+1}} \begin{bmatrix} 1 & \rho_{i,i+1} \\ \rho_{i,i+1} & 1 \end{bmatrix} \tag{5}$$

where $\tau_{i,i+1}$ and $\rho_{i,i+1}$ are the Fresnel coefficient between the i^{th} layer and the next one:

The relationship between the incident and reflected signal at the input port and the transmitted field at the output port is written as follows [18]:

$$\begin{bmatrix} E_i \\ E_r \end{bmatrix} = \left([MM]_{A,1} \cdot \sum_{i=1}^{N} [PM]_i [MM]_{i,i+1} \right) \begin{bmatrix} E_t \\ 0 \end{bmatrix} \tag{6}$$

Due to its infinite extension, the signal propagating in medium B vanishes. The reflection and transmission coefficients of the N layer are obtained by solving equation (6) for the unknowns E_r and E_t [18]:

$$\Gamma = \frac{E_r}{E_i} \tag{7}$$

$$T = \frac{E_t}{E_i} \tag{8}$$

It can be shown that both coefficients are solely dependent on the thickness d, the electric permittivity ε_r of the layers, and the electromagnetic wave's angular frequency. If we assume a wall with N layers, we may compute the amplitude and phase of reflection and transmission coefficients across a given frequency range by adjusting the frequency value in expression (6), which results in a complex spectrum of reflected and transmitted signals represented as [18]:

$$E_r(\omega) = \Gamma(\omega) E_i(\omega) \tag{9}$$

$$E_t(\omega) = T(\omega) E_i(\omega) \tag{10}$$

The time-domain reflected and transmitted signals, $E_r(t)$ and $E_t(t)$, can be estimated using the inverse Fourier transform once the complex spectra of complex spectra $E_r(t)$ and $E_t(t)$ have been obtained. The reflected signal measured by the antenna, $E_r(t)$, is what we are interested in here.

Proposed method for wall parameter estimation

A synthetic TWI time domain signal produced analytically by equation (9) with various wall parameters is displayed to demonstrate the influence of the wall parameters. Figure 2 shows a synthetic TWI time domain with wall parameter variations. The first two peaks in the received time domain signal are caused by reflections from the front and back sides of the wall due to the presence of the wall. The maximum magnitude $P1$ of the first peak changes with ε_r, $P2$ changes with ε_r, d, and the time delay $t2$ of the second peak changes with ε_r and d, but $t1$ remains virtually unchanged. As a result, the wall parameters are related to the maximum amplitude $P1$ and time $t2$.

The wall parameters can be calculated using the maximum amplitude $P1$ and the time $t2$ once a relationship has been established. We treat the problem as a regression problem in order to establish the relationship. A two-stage artificial neural network model for wall parameter estimation is used for this purpose. The schematic diagram of the two-stage artificial neural network model is shown in Fig. 3. In the first stage, the relationship between $P1$ and ε_r will be established after training the input–output sets. The model is the name given to this relationship. If the testing data vector $P1$ is provided, the model predicts ε_r. An artificial neural model with one input layer, one hidden layer of 10 neurons, and one output layer is considered. The features extracted from the received signals are represented by X in ANN. The input is $P1_i$, and the output is ε_{ri}. As a result, data $(P1_i, \varepsilon_{ri})$ are obtained, with i being the i^{th} sample. Some samples are chosen as training data $G = \{(P1_1, \varepsilon_{ri}), \ldots (P1_n, \varepsilon_{rn})\}$, where n is the number of training samples.

https://doi.org/10.1017/S1759078722001131 Published online by Cambridge University Press

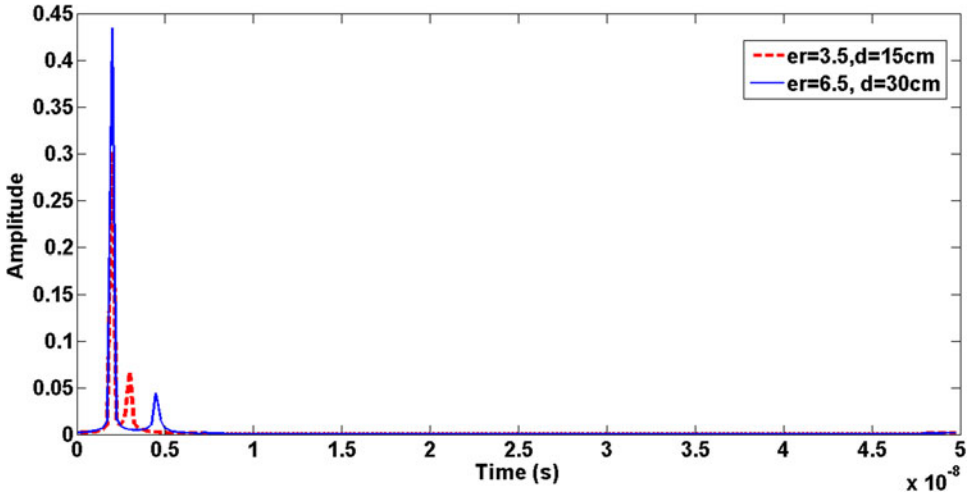

Fig. 2. Plot of synthetic time domain profile with various wall parameters.

In the second stage, the relationship between input ε_r, $t2$, and output d will be established using the artificial neural network model with one input layer, one hidden layer of 10 neurons, and one output layer in the second stage. By taking into account the fact that the parameters are coupled with each other in the wall echoes, the estimation result of one parameter, $\widehat{\varepsilon}_r$, will be used to estimate the other parameter. As a result, data ($t2_i$, ε_{ri}) are obtained, with i being the i^{th} sample. Some samples are chosen as training data $G = \{(t2_1, \varepsilon_{ri}), \ldots. (t2_n, \varepsilon_{rn})\}$, where n is the number of training samples. Once the training is completed, the peak maximum magnitude $P1$ of first peak and time delay $t2$ of the second peak exploited from the time domain profile of material under test can be given as input to trained ANN to get permittivity and thickness of material under test (MUT).

Implementation of ANN with simulation and experimental validation

Simulation results

The proposed method is validated with simulation data before it is used to demonstrate its validity with experimental data. The wall parameter estimation sample has been carried out in accordance with the flow chart shown in Fig. 4 and the steps are given as follows:

Step 1 – data generation: Training data were obtained by varying the relative permittivity, the thickness, and the conductivity between. The 231 data set has been generated by in MATLAB. To obtain the training data, initially a database was created of synthetic TWI time domain signal obtained analytically through equation (4) by varying the relative permittivity between 2 and 7, the thickness between 0.1 and 0.3 m, and the conductivity between 0.0025 and 0.01 S/m. Then, features such as maximum amplitude $P1$ of the first peak and the delay $t2$ of second peak were extracted from synthetic TWI time domain signal.

Step 2 – training: The data set obtained from step 1 has been presented as input vector to the artificial neural network for training. Once the training is completed then the ANN is ready for computation.

Step 3 – testing: The testing data of different samples was obtained from CST simulation. The simulation was done in CST microwave studio to imitate the actual configuration for this purpose. Different samples as rectangular slabs of various thicknesses and permittivity were used in the simulation. For more precision, the simulation is performed using a time domain solver with 10 hexagonal cells per wavelength. On the rectangular slab, a transverse electromagnetic (TEM) wave is generally incident. The boundary conditions are selected in such a way that the structure supports the TEM mode of propagation as the dominant mode in order to allow plane wave propagation.

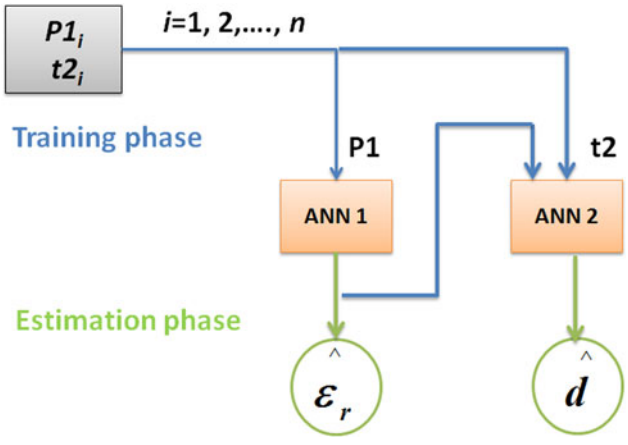

Fig. 3. Schematic diagram of the two-stage artificial neural network model.

Initially, a brick sample with a relative permittivity of 2.5 and a thickness of 10 cm was used as MUT. For the frequency range of 1–3 GHz, the S-parameter $S11$ is computed. The inverse Fourier transform is then used to translate the S parameter from the frequency domain to the time domain. The sample permittivity and thickness were calculated using the proposed scheme and found to be, which is quite near to the given values, resulting in relative permittivity and thickness estimation errors of 4 and 7%, respectively. Furthermore, as indicated in Table 2, the relative permittivity and thickness values of brick samples at

https://doi.org/10.1017/S1759078722001131 Published online by Cambridge University Press

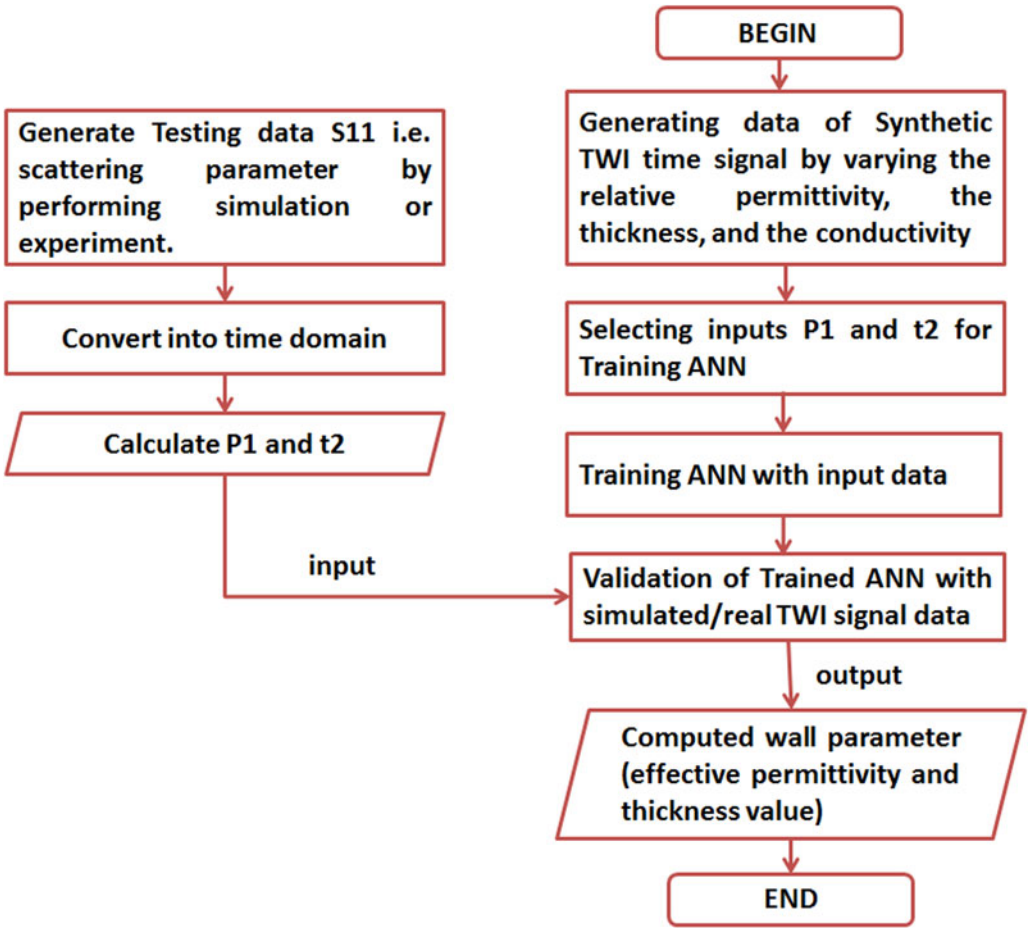

Fig. 4. Flowchart of proposed method for wall parameter estimation.

various thicknesses have been determined. The simulations were also run on various samples of various materials with varying thicknesses, with the estimated results displayed in Table 2. The simulations have also been carried out with different samples of different thicknesses in the frequency range of 3.5–5.5 GHz and their estimated results are shown in Table 3. It can be seen that the proposed scheme successfully estimated the relative permittivity and thickness of various samples with varying thicknesses with high accuracy.

Experimental results

The method is examined using experiment data to demonstrate the efficiency of the estimation approach. The wall parameter estimation sample has been carried out in accordance with the flow chart shown in Fig. 4. First, the 231 training data were generated by varying the relative permittivity, the thickness, and the conductivity between. To obtain the training data, initially a database was created of synthetic TWI time domain signal obtained analytically through equation (4) by varying the relative permittivity

Table 2. Result of estimated relative permittivity and thickness of various samples with varying thicknesses in frequency range 1–3 GHz

Samples	Actual ε_r	Estimated ε_r	Error (%)	Actual d (cm)	Estimated d (cm)	Error (%)
Brick	2.5	2.6	4	15	16.1	7.3
Brick	2.5	2.6	4	20	20.2	1
Brick	2.5	2.6	4	30	29.4	2
Adobe	4.5	4.5	0	15	14.5	3.3
Adobe	4.5	4.7	4.4	20	19.1	4.5
Adobe	4.5	4.7	4.4	30	28.6	4.6
Concrete	6.5	6.7	3	15	15.7	4.6
Concrete	6.5	6.8	4.6	20	19.9	0.05
Concrete	6.5	6.8	4.6	30	28.5	5

https://doi.org/10.1017/S1759078722001131 Published online by Cambridge University Press

Table 3. Result of estimated relative permittivity and thickness of various samples with varying thicknesses in frequency range 3.5–5.5 GHz

Samples	Actual ε_r	Estimated ε_r	Error (%)	Actual d (cm)	Estimated d (cm)	Error (%)
Brick	3.5	4.1	17	10	8.7	13
Concrete	5.5	6.0	9	10	9.7	3
Concrete	5.5	5.9	7.2	20	19.2	4
Concrete	5.5	5.9	7.2	30	29.8	0.6
Glass	6.5	6.3	3	10	9.6	4
Glass	6.5	6.7	3	20	19.2	4
Glass	6.5	6.5	0	30	29.8	0.6

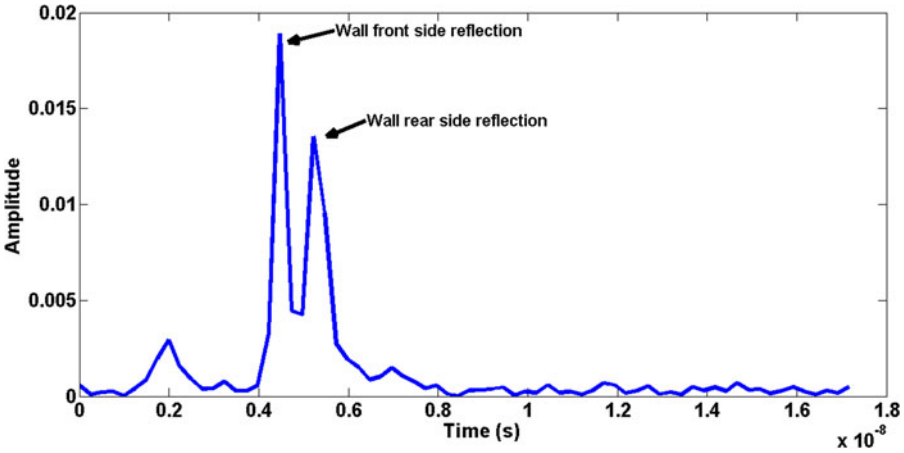

Fig. 5. The time domain plot of real building wall of unknown permittivity and thickness 14.5 cm.

between 2 and 7, the thickness between 0.1 and 0.3 m, and the conductivity between 0.0025 and 0.01 S/m. Then, features such as maximum amplitude $P1$ of the first peak and the delay $t2$ of second peak were extracted from synthetic TWI time domain signal. The dataset presented as input vector to the artificial neural network for training to predict wall parameters. The testing data were obtained with measurement set-up which consists of a horn antenna, which was connected to the vector network analyzer through a coaxial wire. The horn antenna was placed in front of the wall. The background subtraction was done initially to remove antenna mismatch. Initially, a real building wall of unknown permittivity with a thickness of 14.5 cm is considered. $S11$, the scattering parameter, was measured throughout a frequency range of 3.5–5.5 GHz during the experiment. The data measured in frequency domain were converted to time domain by inverse Fourier transform. The time domain plot of real building wall of unknown permittivity and thickness 14.5 cm is shown in Fig. 5. The proposed scheme was used to estimate the wall permittivity and thickness, and their values are shown in Table 4. In addition, as indicated in Table 4, the relative permittivity and thickness values of a different wall with thicknesses of 30 cm and unknown permittivity have also been estimated. It can be observed that the estimated value of thickness of both walls using proposed method was found to be very close to their actual values. In order to check the reliability of the proposed method, the effective permittivity was estimated using pole extraction method [7], as shown in Table 4. As evident, the estimated value of effective permittivity of both walls using proposed method were found to be very close to the values determined using [7].

Our method estimated the wall parameters from the signal, which contained information about the targets on the other side of the wall. Our study's experimental findings showed that our approach is adequately resilient to real-world challenges. Real building materials are often inhomogeneous. The wall can be considered to be homogeneous with an effective permittivity, though, if the inhomogeneities are less in size than the range resolution [3]. It is obvious that with uniform homogeneous walls best results can be obtained. However, we have shown that the approach is capable of handling actual building walls. Obviously, not all possible real-world scenarios are suitable for our method (e.g. with multilayered or strongly inhomogeneous

Table 4. Result of estimated relative permittivity and thickness of two real building walls of different thicknesses

MUT	Parameter estimated using different method	Actual value	Estimated value
Wall 1	Relative permittivity (proposed)	2.5–6	3.5
	Thickness (proposed)	14.5 cm	13.8 cm
	Relative permittivity 2nd method [7]	2.5–6	3.5
Wall 2	Relative permittivity (proposed)	2.5–6	5.6
	Thickness (proposed)	30 cm	30 cm
	Relative permittivity 2nd method [7]	2.5–6	5.4

https://doi.org/10.1017/S1759078722001131 Published online by Cambridge University Press

wall structures). In these cases, identifying the time delays that correspond to the back side of the wall will be more difficult and will almost certainly necessitate the assistance of the radar operator. The proposed method requires time-domain signals as the reference signal with metallic plate and in free-space, respectively. However, these data can be acquired in the laboratory and stored in the memory of a through-wall device.

Conclusion

This research work has been carried out with an intention to develop cost-effective solutions of machine learning-based wall parameter estimation for TWI applications. An effort has been made in this paper to establish a cost-effective and robust wall parameter estimation process with the usage of transmission-line circuit model and artificial neural network. The synthetic TWI signal generated by an equivalent transmission-line circuit model was used to train the artificial neural network. The simulation and experimental results demonstrated that the ANN model can predict the wall parameters accurately and quickly. The proposed scheme estimated wall permittivity and thickness value of real building wall close to the value determined with pole extraction method. The proposed method is simpler and computationally efficient. As only one snapshot is required, the ANN predictor is more suitable for TWRI and can be executed simultaneously in real time. Furthermore, the less stringent frequency requirement makes it more robust.

Acknowledgements. The author would like to thank Prof. P. K. Jain and Dr. Smrity Dwivedi for providing the lab facilities at Indian Institute of Technology (Banaras Hindu University), Varanasi, U.P., India.

Financial support. This research received no specific grant from any funding agency, commercial or not-for-profit sectors.

Conflict of interest. None.

References

1. **Qu L** (2020) Sparse blind deconvolution method for wall parameters estimation. *IEEE Geoscience and Remote Sensing Letters* **19**, 1–5.
2. **Wang G and Amin MG** (2006) Imaging through unknown walls using different standoff distances. *IEEE Transactions on Signal Processing* **54**, 4015–4025.
3. **Protiva P, Mrkvica J and Machác J** (2011) Estimation of wall parameters from time-delay-only through-wall radar measurements. *IEEE Transactions on Antennas and Propagation* **59**, 4268–4278.
4. **Kaushal S, Kumar B and Singh D** (2009) An autofocusing method for imaging the targets for TWI radar systems with correction of thickness and dielectric constant of wall. *International Journal of Microwave and Wireless Technologies* **11**, 15–21.
5. **Liang B, Jin L and Yuan M** (2022) Autofocusing imaging method based on alternating learning of wall parameters and sparse coefficients for through-the-wall radar. *Seventh Asia Pacific Conference on Optics Manufacture and 2021 International Forum of Young Scientists on Advanced Optical Manufacturing (APCOM and YSAOM 2021)*. Shanghai, China: SPIE, pp. 442–447.
6. **Xu Z, Jin T and Dai Y** (2022) Image domain filter for 3-D autofocusing of MIMO plane array in penetration scene. *IEEE Geoscience and Remote Sensing Letters* **19**, 1–5.
7. **Sadeghi S, Mohammadpour-Aghdam K, Ren K, Faraji-Dana R and Burkholder RJ** (2019) A pole-extraction algorithm for wall characterization in through-the-wall imaging systems. *IEEE Transactions on Antennas and Propagation* **67**, 7106–7113.
8. **Chen X and Chen W** (2015) Wall parameters estimation based on support vector regression for through wall radar sensing. *EURASIP Journal on Advances in Signal Processing* **57**, 1–13.
9. **Zhang HM, Zhang YR, Wang FF and An JL** (2015) Application of support vector machines for estimating wall parameters in through-wall radar imaging. *International Journal of Antennas and Propagation* **2015**, 1–8.
10. **Zhang HM, Zhang YR, Wang ZB, Wu ZH and Zhang CX** (2016) An efficient method based on machine learning for estimation of the wall parameters in through-the-wall imaging. *International Journal of Remote Sensing* **37**, 3061–3073.
11. **Ghorbani F and Hossein S** (2021) Simultaneous estimation of wall and object parameters in TWR using deep neural network. *arXiv preprint arXiv*, 2111.04568.
12. **Ghorbani F, Soleimani H and Soleimani M** (2021) Deep learning approach for target locating in through-the-wall radar under electromagnetic complex wall. *arXiv preprint arXiv*, 2102.07990.
13. **Nia BA, Sadeghi S and Flaviis FD** (2022) Using the convolutional neuron network for target localization and wall characterization in the through the wall imaging problem. *2022 16th European Conference on Antennas and Propagation (EuCAP)*. Madrid, Spain: IEEE, pp. 1–3.
14. **Asghar MZ, Abbas M, Zeeshan K, Kotilainen P and Hämäläinen T** (2019) Assessment of deep learning methodology for self-organizing 5g networks. *Applied Sciences* **9**, 2975.
15. **Singh AP, Dwivedi S and Jain PK** (2020) A novel application of artificial neural network for recognition of target behind the wall. *Microwave and Optical Technology Letters* **62**, 152–167.
16. **Kaushal S, Kumar B, Sharma P and Singh D** (2021) Real-time adaptive approach for hidden targets shape identification using through wall imaging system. *Defence Science Journal* **71**, 395–402.
17. **Uthayakumar A, Mohan MP, Khoo EH, Jimeno J, Siyal MY and Karim MF** (2022) Machine learning models for enhanced estimation of soil moisture using wideband radar sensor. *Sensors* **22**, 5810.
18. **Pozar DM** (2011) *Microwave Engineering*, 4th Edn. New York: John Wiley & Sons.

Akhilendra Pratap Singh received Ph.D. degree in electronics engineering from Indian Institute of Technology (Banaras Hindu University), Varanasi, India in 2019 and M.Tech. degree in computer science engineering from ABV Indian Institute of Information Technology and Management, Gwalior, M.P., India in 2012. Currently, he is an Assistant Professor in School of Engineering and Technology at Maharishi University of Information Technology, Lucknow, U.P., India. His main research interests include microwave imaging and antenna.

https://doi.org/10.1017/S1759078722001131 Published online by Cambridge University Press